Double insertions of SMEFT operators in gluon fusion Higgs boson production

Konstantin Asteriadis,[*] Sally Dawson,[†] and Duarte Fontes[‡]

High Energy Theory Group, Department of Physics, Brookhaven National Laboratory, Upton, New York 11973, USA

(Received 5 January 2023; accepted 3 March 2023; published 24 March 2023)

Deviations from the Standard Model (SM) can be parametrized in terms of the SM effective field theory (SMEFT), which is typically truncated at dimension-6. Including higher dimension operators—as well as considering simultaneous insertions of multiple dimension-6 operators—may be necessary in some processes, in order to correctly capture the properties of the underlying UV theory. As a step toward clarifying this in the Higgs boson production in gluon fusion process, we study double insertions of dimension-6 operators in the 1-loop virtual amplitude. We present needed Feynman rules up to $\mathcal{O}(1/\Lambda^4)$ and we numerically study the impact of various approximations to the $\mathcal{O}(1/\Lambda^4)$ expansion.

DOI: 10.1103/PhysRevD.107.055038

I. INTRODUCTION

Current measurements of LHC experiments are in excellent agreement with theoretical predictions, but with uncertainties at the $\mathcal{O}(5\%\text{–}20\%)$ level [1,2]. As a result, the High Luminosity LHC program will be focused on high precision measurements. It is expected that the experimental uncertainties will reduced to $\mathcal{O}(1\%)$ for many observables [3]. This requires precise theoretical Standard Model (SM) predictions, but also precise computations in specific beyond the Standard Model (BSM) scenarios to describe potentially emerging small non-SM signatures. A more general approach is also possible; BSM physics which contains no new light particles and which respects the SM gauge symmetries can be parametrized using the Standard Model effective field theory (SMEFT) [4]. This consists of an expansion around the SM Lagrangian $\mathcal{L}_{\rm SM}$ in terms of an infinite tower of higher dimension operators,

$$\mathcal{L} = \mathcal{L}_{\rm SM} + \sum_{d=5}^{\infty}\sum_i \frac{C_i^d O_i^d}{\Lambda^{d-4}}, \tag{1}$$

where Λ is chosen to be the scale of new physics, O_i^d are operators of dimension d, and C_i^d the corresponding dimensionless SMEFT Wilson coefficients (WC). Fits to the latter have been made using Higgs, diboson, electroweak precision, and top data [5–8]. Such analyses are usually done by terminating the series in Eq. (1) after dimension-6 operators. Yet, the need for precision calls for an investigation beyond $\mathcal{O}(1/\Lambda^2)$. At the next nontrivial order, this includes studying the impact of dimension-8 SMEFT operators, but also double insertions of dimension-6 operators [9–17]. An amplitude, A_i, for a lepton number conserving process can be parametrized in the SMEFT as a power series in $1/\Lambda^2$,

$$A_i \sim A_{i,\rm SM} + \sum_j \frac{C_j^6}{\Lambda^2}\alpha_{ij}^6 + \sum_{j,k}\frac{C_j^6 C_k^6}{\Lambda^4}\alpha_{ijk}^{6^2} + \sum_j \frac{C_i^8}{\Lambda^4}\alpha_{ij}^8 + \mathcal{O}(1/\Lambda^6), \tag{2}$$

where the α coefficients are process dependent. The terms proportional to $C_j^6 C_k^6/\Lambda^4$ are the double insertions of interest here. The amplitude-squared corresponding to a cross section is then expanded generically as,

$$|A_i|^2 \sim |A_{i,\rm SM}|^2 + \frac{1}{\Lambda^2}\sum_j 2\,\mathrm{Re}(A_{i,\rm SM}^* C_j^6 \alpha_{ij}^6) + \frac{1}{\Lambda^4}\left[\sum_{j,k}(C_j^6 C_k^{6*}\alpha_{ij}^6\alpha_{ik}^{6*} + 2\,\mathrm{Re}(A_{i,\rm SM}^* C_j^6 C_k^6 \alpha_{ijk}^{6^2})) + \sum_j 2\,\mathrm{Re}(A_{i,\rm SM}^* C_j^8 \alpha_{ij}^8)\right] + \mathcal{O}(1/\Lambda^6). \tag{3}$$

[*]kasteriad@bnl.gov
[†]dawson@bnl.gov
[‡]dfontes@bnl.gov

If a coefficient is well constrained by data, it may be sufficient to retain only the $\mathcal{O}(1/\Lambda^2)$ contributions to observables. This is typically the case in fits to electroweak precision observables [18–20]. However, for most of the SMEFT coefficients contributing to predictions for LHC observables, the $\mathcal{O}(1/\Lambda^4)$ terms play an important role. Global fits [5–8] include the first term on the second line of Eq. (3) (required to make the cross sections positive-definite), but the other terms of $\mathcal{O}(1/\Lambda^4)$ are more subtle. For tree-level processes, the second term on the second line of Eq. (3) (which corresponds to a double insertion) is easily included [21,22] and can have important numerical effects [23]. The dimension-8 contributions [first term on the third line of Eq. (3)] have been studied in only a few special cases and the numerical importance of these terms is not known in general [9–11,24]. In the case where the new physics that generates the SMEFT coefficients corresponds to a strongly interacting theory, it has been argued that the dimension-8 contributions are small [25].

In the following, we present a preliminary investigation of the impact of double insertions on the inclusive gluon fusion Higgs boson production process. This production channel has recently been calculated in the SM to N^{3}LO QCD [26–28]. In the SMEFT, the NLO result with single insertions of dimension-6 operators is well known [29–33]. Gluon fusion Higgs production has also been calculated to all orders in v^2/Λ^2 using the GeoSMEFT approach [34,35]. Here, we present a study of the 1-loop contributions to the $gg\to h$ amplitude including all terms of $\mathcal{O}(1/(16\pi^2\Lambda^4))$ and we investigate the numerical effects of double insertions of a consistent subset of dimension-6 SMEFT operators.

The paper is organized as follows. Section II contains a brief description of the SMEFT to $\mathcal{O}(1/\Lambda^4)$. The 1-loop calculation of $gg\to h$ to $\mathcal{O}(1/(16\pi^2\Lambda^4))$ is presented in Sec. III, including the insertion of two dimension-6 operators in the 1-loop amplitude and the required counterterm for the $gg\to h$ process corresponding to the dimension-8 $(\varphi^\dagger\varphi)^2 G^{A,\mu\nu}G^B_{\mu\nu}$ operator. Numerical effects of the double insertions are investigated in Sec. IV, along with a discussion of the potential effects of neglected contributions. Finally, we conclude in Sec. V with a discussion of the path forward to a more complete study of the impact of $\mathcal{O}(1/\Lambda^4)$ effects.

II. SMEFT TO $\mathcal{O}(\Lambda^{-4})$

We start by presenting the pieces of the dimension-6 SMEFT Lagrangian (in the Warsaw basis [36]) which are relevant for the calculation of the virtual 1-loop $gg\to h$ diagrams containing double insertions. All the remaining necessary terms of the Lagrangian can be found in Ref. [37]. In the end of this section, we present the relationships up to $\mathcal{O}(1/\Lambda^4)$ between the original parameters of the Lagrangian and our input parameters [24].

We neglect finite contributions from dimension-8 terms. Although such contributions enter in the cross section at the same order as double insertions of dimension-6 operators, they can be treated separately, as they are not required to obtain a gauge-independent result. Yet, the dimension-8 operators are in general required to absorb ultraviolet (UV) divergences of $\mathcal{O}(1/\Lambda^4)$. There is a single dimension-8 operator that can be used to this end [38,39],

$$\frac{C_{G^2\varphi^4}}{\Lambda^4}(\varphi^\dagger\varphi)^2 G^A_{\mu\nu}G^{A\mu\nu}. \tag{4}$$

When renormalizing the theory, the counterterm $\delta C_{G^2\varphi^4}$ is generated from Eq. (4). Below, we present the result $\delta C_{G^2\varphi^4}$ using minimal subtraction. We work in minimal subtraction, which amounts to dropping all poles. A complete understanding of dimension-8 renormalization in the SMEFT, including fermionic operators, does not yet exist, although significant progress has been made in understanding the bosonic operators [40–44].

A. Lagrangian and field redefinitions

The relevant pieces of the dimension-6 SMEFT Lagrangian can be grouped into three terms,

$$\mathcal{L}_{\text{Higgs}} + \mathcal{L}_{\text{QCD}} + \mathcal{L}_{\text{fermions}}. \tag{5}$$

The first one is the Higgs Lagrangian,

$$\begin{aligned}\mathcal{L}_{\text{Higgs}} &= (D^\mu\varphi)^\dagger(D_\mu\varphi) + \mu^2\varphi^\dagger\varphi - \frac{\lambda}{2}(\varphi^\dagger\varphi)^2 \\ &\quad + \frac{1}{\Lambda^2}[C_\varphi(\varphi^\dagger\varphi)^3 + C_{\varphi\Box}(\varphi^\dagger\varphi)\Box(\varphi^\dagger\varphi) \\ &\quad + C_{\varphi D}(\varphi^\dagger D^\mu\varphi)^*(\varphi^\dagger D_\mu\varphi)],\end{aligned} \tag{6}$$

where φ represents the Higgs doublet, which we parametrize as

$$\varphi = \begin{pmatrix} \varphi^+ \\ \frac{1}{\sqrt{2}}(v_T + h + i\varphi^0) \end{pmatrix}. \tag{7}$$

Here, v_T is the vacuum expectation value (vev) that minimizes the Higgs potential in the presence of the SMEFT operators, and h, φ^0, and φ^+ represent the Higgs, the neutral Goldstone, and the charged Goldstone boson fields, respectively. The second term in Eq. (5) is the QCD Lagrangian,

$$\begin{aligned}\mathcal{L}_{\text{QCD}} &= -\frac{1}{4}G^A_{\mu\nu}G^{A\mu\nu} + \frac{C_{\varphi G}}{\Lambda^2}(\varphi^\dagger\varphi)G^A_{\mu\nu}G^{A\mu\nu} \\ &\quad + \frac{C_G}{\Lambda^2}f_{ABC}G^{A\nu}_{\mu}G^{B\rho}_{\nu}G^{C\mu}_{\rho},\end{aligned} \tag{8}$$

with

$$G^A_{\mu\nu} = \partial_\mu g^A_\nu - \partial_\nu g^A_\mu - g_s f^{ABC} g^B_\mu g^C_\nu, \tag{9}$$

where g^A_μ is the gluon field. Finally, $\mathcal{L}_{\text{fermions}}$ is the fermionic Lagrangian,

$$\mathcal{L}_{\text{fermions}} = -Y_u \bar{q}_L \varphi d_R + \left[\frac{C_{t\varphi}}{\Lambda^2}(\varphi^\dagger\varphi)(\bar{q}_L\tilde{\varphi}u_R) + \text{H.c.}\right] + \frac{C_{ll}}{\Lambda^2}(\bar{l}_L\gamma_\mu l_L)(\bar{l}'_L\gamma_\mu l'_L) + \frac{C^{(3)}_{\varphi l}}{\Lambda^2}\varphi^\dagger i\overleftrightarrow{D}^a_\mu\varphi(\bar{l}_L\tau^a\gamma_\mu l_L), \tag{10}$$

with $q^{\mathrm{T}}_L = (u_L, d_L)$, $l^{\mathrm{T}}_L = (\nu_L, e_L)$, $\tilde{\varphi} = i\sigma_2\varphi^*$, and we retain only the top quark contributions.

To ensure that all fields have canonical kinetic terms, we need to perform the following shifts,

$$h \to hR^{-1}_\phi, \tag{11a}$$

$$\varphi^0 \to \varphi^0 R^{-1}_{\varphi^0}, \tag{11b}$$

$$g^A_\mu \to g^A_\mu R^{-1}_g, \tag{11c}$$

where

$$R_\varphi = 1 - \frac{v_T^2}{\Lambda^2}X_h - \frac{v_T^4}{2\Lambda^4}X_h^2 + \mathcal{O}(\Lambda^{-6}), \tag{12a}$$

$$R_{\varphi^0} = 1 + \frac{v_T^2}{4\Lambda^2}C_{\varphi D} - \frac{v_T^4}{32\Lambda^4}C^2_{\varphi D} + \mathcal{O}(\Lambda^{-6}), \tag{12b}$$

$$R_g = 1 - \frac{v_T^2}{\Lambda^2}C_{\varphi G} - \frac{v_T^4}{2\Lambda^4}C^2_{\varphi G} + \mathcal{O}(\Lambda^{-6}), \tag{12c}$$

with X_h in Eq. (12a) defined as

$$X_h \equiv C_{\varphi\Box} - \frac{C_{\varphi D}}{4}. \tag{13}$$

B. Input parameters

We choose as independent parameters

$$G_F, \quad \alpha_s, \quad M_Z, \quad M_W, \quad M_h, \quad m_t, \tag{14}$$

where G_F is the Fermi constant, α_s is the strong coupling constant and $M_Z(M_W), M_h$, and m_t are the gauge boson, Higgs, and top masses.

The expression for v_T can be determined through the amplitude for muon decay, including double insertions of dimension-6 operators. Assuming flavor universality of the WCs

$$G_F = \frac{1}{\sqrt{2}v_T^2} + \frac{\sqrt{2}}{\Lambda^2}\left(C^{(3)}_{\varphi l} - \frac{1}{2}C_{ll}\right) + \frac{v_T^2}{\sqrt{2}}\frac{(C^{(3)}_{\varphi l})^2}{\Lambda^4}, \tag{15}$$

which can be inverted to yield

$$v_T = \frac{1}{(\sqrt{2}G_F)^{\frac{1}{2}}} + \frac{2C^{(3)}_{\varphi l} - C_{ll}}{2(\sqrt{2}G_F)^{\frac{3}{2}}\Lambda^2} + \frac{16\left(C^{(3)}_{\varphi l}\right)^2 - 12C^{(3)}_{\varphi l}C_{ll} + 3C^2_{ll}}{8(\sqrt{2}G_F)^{\frac{5}{2}}\Lambda^4}. \tag{16}$$

The parameters μ^2 and λ are fixed by the requirement that the coefficient of the Higgs tadpole contribution vanishes (i.e. that v_T is the true vev) and that the mass of the Higgs field in the Lagrangian is given by M_h. Using also Eq. (16), we find

$$\mu^2 = \frac{M_h^2}{2} + \frac{3C_\varphi - 4\sqrt{2}X_h G_F M_h^2}{8G_F^2\Lambda^2} + \frac{(2C^{(3)}_{\varphi l} - C_{ll})(3\sqrt{2}C_\varphi - 4X_h G_F M_h^2)}{8G_F^3\Lambda^4}, \tag{17}$$

$$\lambda = G_F M_h^2\sqrt{2} + \frac{3\sqrt{2}C_\varphi + 2(C_{ll} - 2C^{(3)}_{\varphi l} - 2X_h)G_F M_h^2}{2G_F\Lambda^2} - \frac{3C_\varphi(C_{ll} - 2C^{(3)}_{\varphi l}) + \sqrt{2}(C^{(3)}_{\varphi l})^2 G_F M_h^2}{2G_F^2\Lambda^4}. \tag{18}$$

The top quark Yukawa coupling is determined by requiring that the mass of the top-quark field in Eq. (10) is given by m_t,

$$Y_t = \sqrt{2}(\sqrt{2}G_F)^{\frac{1}{2}}m_t \times\left[1 - \frac{2C^{(3)}_{\varphi l} - C_{ll}}{2(\sqrt{2}G_F)\Lambda^2} - \frac{8(C^{(3)}_{\varphi l})^2 - 4C^{(3)}_{\varphi l}C_{ll} + C^2_{ll}}{8(\sqrt{2}G_F)^2\Lambda^4}\right] + \frac{C_{t\varphi}}{2(\sqrt{2}G_F)\Lambda^2}\left[1 + \frac{2C^{(3)}_{\varphi l} - C_{ll}}{(\sqrt{2}G_F)\Lambda^2}\right]. \tag{19}$$

Finally, g_s^2 can be related to $4\pi\alpha_s$ through the inverse transformation of Eq. (11c) and we find

$$g_s = \bar{g}_s\left[1 - \frac{1}{\sqrt{2}G_F}\frac{C_{\varphi G}}{\Lambda^2} - \frac{1}{4G_F^2}\frac{C_{\varphi G}\left(C_{\varphi G} + 4C^{(3)}_{\varphi l} - 2C_{ll}\right)}{\Lambda^4}\right], \tag{20}$$

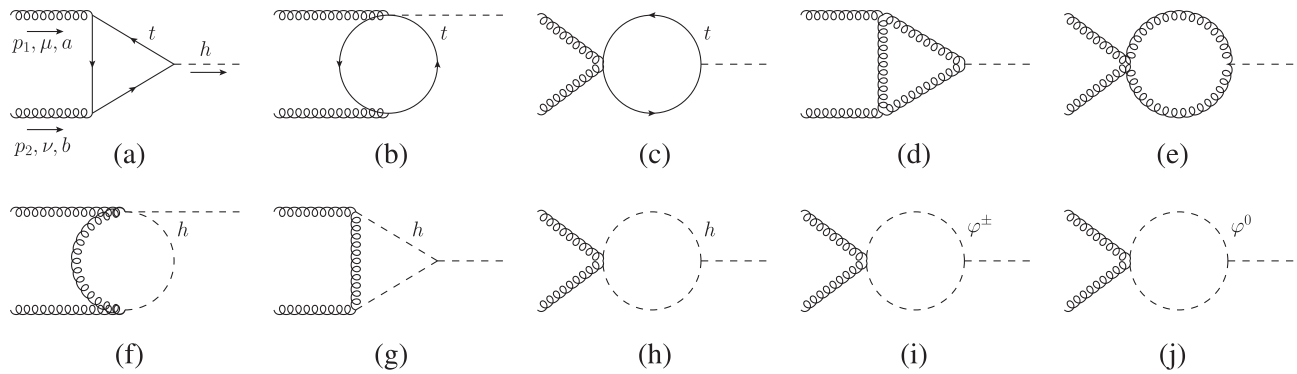

FIG. 1. Virtual 1-loop contributions to the gluon fusion to Higgs amplitude including contributions from both single and double insertions of dimension-6 SMEFT operators. Conventions used throughout the paper concerning 4-momenta, Lorentz indices and color indices are shown in diagram (a). Note that diagrams (a), (b), and (f) also contribute with crossed initial states (not shown for compactness).

where we defined

$$\bar{g}_s \equiv \sqrt{4\pi\alpha_s}. \tag{21}$$

III. CALCULATION

We now describe the 1-loop calculation of the $gg \to h$ amplitude to $\mathcal{O}(1/(16\pi^2\Lambda^4))$. The Feynman rules accurate to $\mathcal{O}(1/\Lambda^4)$ that are relevant for our calculation are given in Appendix B. Lorentz and gauge invariance imply that at any order, the amplitude for $g^A(p_1^\mu)g^B(p_2^\nu) \to h$ must have the form,

$$A^{\mu\nu}(p_1, p_2) = i\delta_{AB}(p_1^\nu p_2^\mu - p_1 \cdot p_2 g^{\mu\nu})\sum_i F_i, \tag{22}$$

where, up to 1-loop,

$$\sum_i F_i = F_0 + F_{\mathrm{V}} + F_{\mathrm{CT}}, \tag{23}$$

with F_0 representing the tree-level SMEFT contribution, F_{V} the virtual 1-loop amplitude and F_{CT} the total counterterm.

The tree-level contribution is given by

$$F_0 = \frac{4C_{\varphi G}}{(\sqrt{2}G_F)^{\frac{1}{2}}\Lambda^2} + \frac{C_{\varphi G}}{(\sqrt{2}G_F)^{\frac{3}{2}}\Lambda^4} \times [8C_{\varphi G} + 4X_h + 4C_{\varphi l}^{(3)} - 2C_{ll}]. \tag{24}$$

F_{V} is computed from the diagrams shown in Fig. 1, using the software FeynMaster [45–53]. We use the true vev up to 1-loop order [54] and we work in the Parameter Renormalized tadpole scheme [55,56]. Analytic results for F_{V} can be found in the auxiliary file submitted with this paper. Finally, F_{CT} is determined by identifying the original parameters and fields in Eqs. (4) and (5) as bare parameters (with index "(0)") and by expanding them into renormalized quantities,

$$h_{(0)} = \left(1 + \frac{1}{2}\delta Z_h\right)h, \tag{25a}$$

$$g_{(0)}^{A,\mu} = \left(1 + \frac{1}{2}\delta Z_g\right)g^{A,\mu}, \tag{25b}$$

$$G_{F(0)} = (1 + \delta G_F)G_F, \tag{25c}$$

$$C_{X(0)} = C_X + \delta C_X, \tag{25d}$$

where C_X represents a generic WC. The expression for F_{CT} is given in Appendix A.[1]

This allows us to determine $\delta C_{G^2\varphi^4}$ by requiring Eq. (23) be free from divergences. We work in dimensional regularization, using $D = 4 - 2\epsilon$ for the spacetime dimension, and fix the counterterms of the WCs in the minimal subtraction scheme [57,58]. We perform the calculation in two independent ways: (i) we subtract known infrared (IR) poles using results of Ref. [59]; and (ii) we use Package-X [60,61] and consider only UV poles.

It is sufficient to compute the counterterms in Eq. (A2) to order $\mathcal{O}(1/\Lambda^2)$, since Eq. (A2) is already $\mathcal{O}(1/\Lambda^2)$. δZ_h and δZ_g can be computed from the Higgs and gluon self energies at 1-loop, respectively; explicit expressions can be found in Appendix A. δG_F is given by

$$\delta G_F = -\frac{1}{16\pi^2}\frac{G_F}{\sqrt{2}}\Delta r_{\mathrm{SM}} - \frac{1}{16\pi^2}\frac{1}{\Lambda^2}\Delta r_{\mathrm{EFT}} + \frac{1}{2}\left(2C_{\varphi l}^{(3)} - C_{ll}\right)\frac{\Delta r_{\mathrm{SM}}}{16\pi^2\Lambda^2} + \frac{1}{2}\left(2\delta C_{\varphi l}^{(3)} - \delta C_{ll}\right)\frac{\sqrt{2}}{G_F\Lambda^2}, \tag{26}$$

[1] As discussed in Sec. II, we ignore finite effects from dimension-8 operators (i.e., we set the renormalized WC $C_{G^2\varphi^4}$ to zero).

where the expressions for $\Delta r_{\rm SM}$ and $\Delta r_{\rm EFT}$ can be found in Appendix D of Ref. [62]. The contributions from $\delta C_{\varphi l}^{(3)}$ and δC_{ll} cancel when Eq. (26) is used in Eq. (A2). The contribution to $\delta C_{\varphi G}$ of $\mathcal{O}(1/\Lambda^2)$ can be obtained from Refs [63–65]; we confirmed their result by requiring that Eq. (22) be finite to $\mathcal{O}(1/\Lambda^2)$ and present it in Eq. (A1). Combining these elements, we find the expression for $\delta C_{G^2\varphi^4}$ given in Eq. (A5).

TABLE I. Numerical results for linear coefficients a_i and coefficients b_{ij} of pairs of SMEFT WCs, cf. Eq. (27). Results are shown with (third column) or without (second column) double insertions. In the fourth column we show the ratio of *single* coefficients over *double* coefficients. Ratios given as rational numbers are exact. Numerical values for physical parameters are reported in Sec. IV. See text for further details.

$\frac{10^{-4}}{\mathrm{GeV}^2}\cdot a_i$	Linear
$C_{\varphi l}^{(3)}$	−12.13
C_{ll}	6.06
$C_{\varphi\Box}$	12.13
$C_{\varphi D}$	−3.03
$C_{t\varphi}$	−12.28
C_{tG}	19.35

$\frac{10^{-10}}{\mathrm{GeV}^4}\cdot b_{ij}$	Single	Double	Ratio
$C_{\varphi l}^{(3)2}$	0.3678	−0.3678	−1
$C_{ll}C_{\varphi l}^{(3)}$	−0.3678	…	…
C_{ll}^2	0.0919	…	…
$C_{\varphi\Box}C_{\varphi l}^{(3)}$	−0.7355	…	…
$C_{\varphi\Box}C_{ll}$	0.3678	…	…
$C_{\varphi\Box}^2$	0.3678	1.4711	1/4
$C_{\varphi D}C_{\varphi l}^{(3)}$	0.1839	…	…
$C_{\varphi D}C_{ll}$	−0.0919	…	…
$C_{\varphi D}C_{\varphi\Box}$	−0.1839	−0.7355	1/4
$C_{\varphi D}^2$	0.0230	0.0919	1/4

$\frac{10^{-10}}{\mathrm{GeV}^4}\cdot b_{ij}$	Single	Double	Ratio
$C_{t\varphi}C_{\varphi l}^{(3)}$	0.7447	−0.7447	−1
$C_{t\varphi}C_{ll}$	−0.3723	0.3723	−1
$C_{t\varphi}C_{\varphi\Box}$	−0.7447	−1.4893	1/2
$C_{t\varphi}C_{\varphi D}$	0.1862	0.3723	1/2
$C_{t\varphi}^2$	0.3769	0.3769	1
$C_{tG}C_{\varphi l}^{(3)}$	−1.1732	−1.1732	1
$C_{tG}C_{ll}$	0.5866	0.5866	1
$C_{tG}C_{\varphi\Box}$	1.1732	2.3465	1/2
$C_{tG}C_{\varphi D}$	−0.2933	−0.5866	1/2
$C_{tG}C_{t\varphi}$	−1.1878	−0.0661	17.97
${C_{tG}}^2$	0.9357	1.3909	0.6727

IV. IMPACT OF DOUBLE INSERTIONS

To study the impact of double insertions on the 1-loop amplitude of the gluon fusion process, we compute the amplitude squared in two ways: (i) we truncate the amplitude at $\mathcal{O}(1/\Lambda^2)$ and then compute the amplitude squared; and (ii) we compute the amplitude to $\mathcal{O}(1/\Lambda^4)$ and then truncate the amplitude squared at $\mathcal{O}(1/\Lambda^4)$. The first truncation is not sensitive to the double insertions of the dimension-6 operators, and we label it as "*single*." The second truncation is sensitive to the double insertions of SMEFT operators, and we label it as "*double*." We note that the latter is in fact a complete computation of the virtual amplitude up to $\mathcal{O}(1/\Lambda^4)$ at 1-loop, neglecting finite contributions from dimension-8 operators. Since the WC $C_{\varphi G}$ contributes at tree-level, the double insertions proportional to $C_{\varphi G}$ require the computation of 2-loop virtual graphs with single insertions of dimension-6 operators, along with 1-loop virtual graphs proportional to $C_{\varphi G}$ to obtain an IR finite result.

As a first step in understanding the relevance of double insertions, we consider a scenario where $C_{\varphi G}$ is generated at loop level and thus can be consistently set to zero after renormalization. This is a realistic scenario from a model building point of view. At tree-level, scalars, vectorlike quarks, and vector particles in arbitrary representations that contribution to the dimension-6 SMEFT Lagragian do not generate $C_{\varphi G}$ contributions [66]. It is interesting to note that vectorlike quarks generate $C_{\varphi G}$ at 1-loop consistent with our assumption. When we set $C_{\varphi G}=0$, there are no real corrections and we can study the numerical effects of the double insertions from the remaining operators using our finite results for the renormalized amplitude to construct a cross section normalized to the SM result.[2]

For the numerical results reported below, we use $M_h = 125$ GeV, $M_W = 80.377$ GeV, $M_Z = 91.1876$ GeV, $m_t = 172$ GeV, $G_F = 1.166\times10^{-5}$ GeV^{-2}, and $\alpha_s = 0.1179$. The renormalization scale μ is chosen to be equal to the Higgs mass M_h. Finally, we write the virtual amplitude squared as,

$$\left|\frac{\sum_i F_i}{F_{\rm SM}}\right|^2 \equiv 1 + \sum_i a_i \frac{C_i}{\Lambda^2} + \sum_{i,j\le i} b_{ij}\frac{C_i C_j}{\Lambda^4}. \quad (27)$$

In the $C_{\varphi G} = 0$ limit that we are working in,

$$\mu_{ggh} \equiv \frac{\sigma(gg\to h)}{\sigma(gg\to h)|_{\rm SM}} = \left|\frac{\sum_i F_i}{F_{\rm SM}}\right|^2. \quad (28)$$

Numerical results for a_i and b_{ij} in the 2 expansions at $\mathcal{O}(1/\Lambda^4)$ are presented in Table I.

[2]We have explicitly checked the gauge independence of our results.

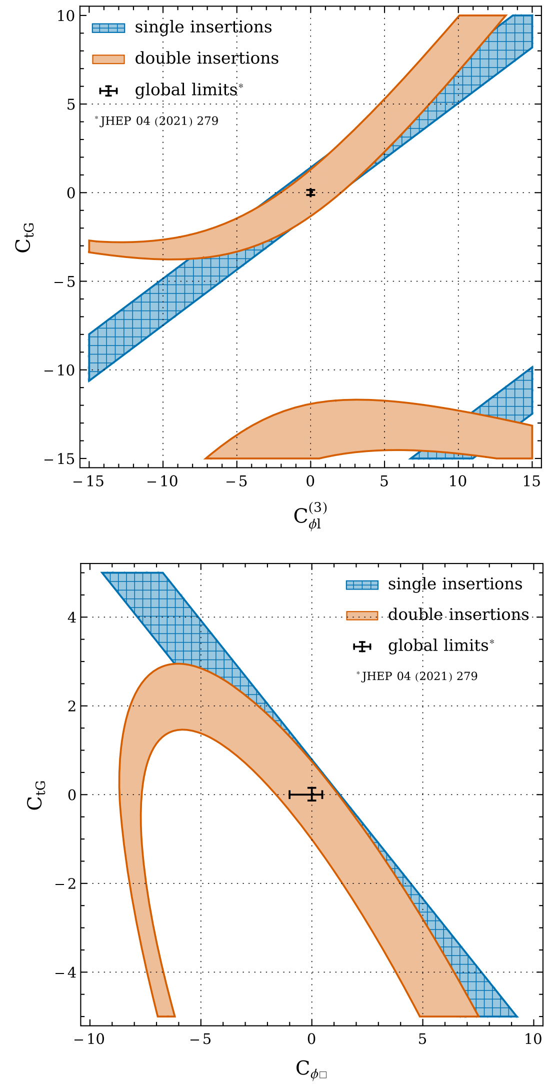

FIG. 2. Regions where $|\mu_{ggh} - 1| < 5\%$ are shown for single insertions (squared blue) and double insertions (orange). The limits from global fits to individual operators at 95% C.L. are denoted by the black cross [5,6,8]. The WCs not shown are varied over values allowed by the 95% C.L. fits to individual coefficients of Ref. [5].

We first note that some contributions that contain C_{ll} or $C^{(3)}_{\varphi l}$ are present in the *single* but vanish in the *double* setup. From the Feynman diagrams shown in Fig. 1 it can be easily seen that these contributions are proportional to $1/(R^2_\varphi v^2_T)$, which vanishes in the *double* expansion. Consequently, the functional dependence of the amplitude on these WCs in the two expansions is quite different; for example, we show this for the combination of $C^{(3)}_{\varphi l}$ and C_{tG} in the upper plot in Fig. 2. In this figure we show the regions where $|\mu_{ggh} - 1|$ is less than 5%. For a given value of $C^{(3)}_{\varphi l}$ and C_{tG}, the remaining coefficients C_{ll}, $C_{\varphi\Box}$, $C_{\varphi D}$, and $C_{t\varphi}$ are varied over the region allowed by the 95% C.L.

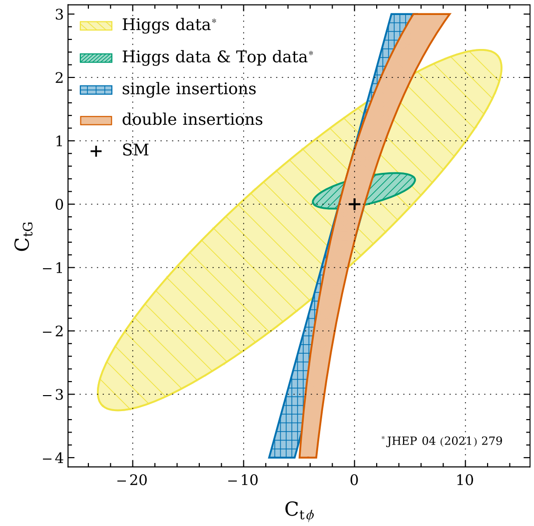

FIG. 3. Allowed parameter space from a 2-parameter fit to $C_{t\varphi}$ and C_{tG}. Yellow (hashed) and green (fine hashed) ellipses show constraints from linear fits at 95% C.L. to Higgs data and Higgs plus top data respectively [6]. Regions where $|\mu_{ggh} - 1| < 5\%$ are shown for single insertions (squared blue) and double insertions (orange). The WCs not shown are varied over values allowed by the 95% C.L. fits to individual coefficients of Ref. [5].

individual fits of Ref. [6].[3] It is clear that the difference between the *single* and *double* insertion expansions has no phenomenological relevance, since the values of the parameters plotted are excluded by fits to Higgs data [5,6,8]. We do not show it explicitly, but we have checked that the same conclusion holds for all other combinations that include C_{ll} and/or $C^{(3)}_{\varphi l}$.

We also observe a nontrivial change in the coefficient of C_{tG} and we show a fit in combination with $C_{\varphi\Box}$ to the value of the SM amplitude squared in Fig. 2 (bottom). Also in this case, significant differences between *single* and *double* expansions only occur for values of the WCs far beyond current single parameter limits [6].

The biggest change is in the coefficient of $C_{tG}C_{t\varphi}$. For this combination of WCs, the allowed parameter space is available in Ref. [6] from 2-parameter fits to Higgs and Higgs plus top data at 95% C.L. In Fig. 3, we show these regions together with a fit to $|\mu_{ggh} - 1| < 5\%$. The difference in the results for *single* and *double* expansions is small and demonstrates the power of including top data in the fits. While fits to Higgs data alone show a small sensitivity to the expansion, when top data is included with the Higgs

[3]Limits used in all figures for WCs not shown explicitly are $-0.5 \le 10^2 \cdot C_{ll} \le 1.9$, $-1.0 \le 10^2 \cdot C^{(3)}_{\varphi l} \le 0.3$, $-1.0 \le C_{\varphi\Box} \le 0.5$, $-2.3 \le 10^2 \cdot C_{\varphi D} \le 0.3$, $-1.0 \le C_{t\varphi} \le 0.8$, and $-1.3 \le 10 \cdot C_{tG} \le 1.5$.

data, there is again no difference between the two expansions in the region allowed by global fits.[4]

V. CONCLUSIONS

We computed the 1-loop amplitude for the gluon fusion process $gg \to h$ including all contributions of dimension-6 operators up to $\mathcal{O}(1/(16\pi^2\Lambda^4))$. This includes double insertions of dimension-6 operators and the relationships between parameters in the SMEFT Lagrangian and physical observables to this order. We derived the necessary Feynman rules that are valid up to $\mathcal{O}(1/\Lambda^4)$ and determined the required counterterm to obtain a UV finite result at this order. For our numerical studies, we considered the limit $C_{\varphi G} = 0$ which ensures that there are no infrared singularities. We note that this is a well-motivated scenario, since in many BSM models $C_{\varphi G}$ is only generated at 1-loop level. We then compared the gluon fusion cross section in different expansions up to $\mathcal{O}(1/\Lambda^4)$ and found that the impact of the double insertions is negligible for values of the WCs allowed by global fits and neglecting the unknown dimension-8 contributions.

An extension of this study including the effects of $C_{\varphi G}$ and double insertions would require 2-loop virtual amplitudes with up to two insertions of dimension-6 SMEFT operators as well as real-virtual and double real emission contributions. We leave this exercise for future investigations [67].

Digital data associated with this research is contained in the auxiliary file attached to this paper.

ACKNOWLEDGMENTS

We thank Pier Paolo Giardino, Guilherme Guedes, Matt Sullivan, and Robert Szafron for useful discussions. The research of K. A., S. D., and D. F. is supported by the United States Department of Energy under Grant Contract No. DE-SC0012704.

APPENDIX A: COUNTERTERMS

Here, we collect results related to the renormalization. In what follows, all results are written in the Feynman gauge and, unless explicitly stated otherwise, ϵ represents $\epsilon_{\rm UV}$ (i.e., a UV pole).

The counterterm $\delta C_{\varphi G}$ receives contributions of $\mathcal{O}(1/\Lambda^4)$. The bosonic contributions of $\mathcal{O}(1/\Lambda^4)$ are given in Ref. [42], while the fermionic contributions are unknown. We denote the total $\mathcal{O}(1/\Lambda^4)$ contribution to $\delta C_{\varphi G}$ as $\delta C^8_{\varphi G}$ and the $\mathcal{O}(1/\Lambda^2)$ contribution as $\delta C^6_{\varphi G}$,

$$\begin{aligned}\epsilon\delta C_{\varphi G} &= \epsilon\left[\delta C^6_{\varphi G} + \frac{1}{\sqrt{2}G_F}\frac{\delta C^8_{\varphi G}}{\Lambda^2}\right]\\ &= -\frac{\sqrt{\alpha_s G_F}m_t}{2^{\frac{5}{4}}\pi^{\frac{3}{2}}}C_{tG} + \frac{3\sqrt{2}G_F(M_h^2+2m_t^2-2M_W^2-M_Z^2)-28\pi\alpha_s}{16\pi^2}C_{\varphi G} + \epsilon\frac{1}{\sqrt{2}G_F}\frac{\delta C^8_{\varphi G}}{\Lambda^2}.\end{aligned} \tag{A1}$$

The quantity $F_{\rm CT}$ defined in Eq. (23) is given by

$$\begin{aligned}F_{\rm CT} = &\frac{2}{(\sqrt{2}G_F)^{\frac{1}{2}}}\frac{2\delta C^6_{\varphi G}+C_{\varphi G}(\delta Z_h+2\delta Z_g-\delta G_F)}{\Lambda^2} + \frac{4}{(\sqrt{2}G_F)^{\frac{3}{2}}}\frac{\delta C^8_{\varphi G}}{\Lambda^4}\\ &+\frac{1}{2(\sqrt{2}G_F)^{\frac{3}{2}}\Lambda^4}\Big[8\delta C_{G^2\varphi^4} + 8C_{\varphi\Box}\delta C^6_{\varphi G} - 2C_{\varphi D}\delta C^6_{\varphi G} + 32C_{\varphi G}\delta C^6_{\varphi G} + 8C^{(3)}_{\varphi l}\delta C^6_{\varphi G} - 4C_{ll}\delta C^6_{\varphi G} + 8C_{\varphi G}\delta C^{(3)}_{\varphi l}\\ &-4C_{\varphi G}\delta C_{ll} + 3C_{\varphi D}C_{\varphi G}\delta G_F - 24C^2_{\varphi G}\delta G_F - 12C_{\varphi G}C^{(3)}_{\varphi l}\delta G_F + 6C_{\varphi G}C_{ll}\delta G_F - 2C_{\varphi D}C_{\varphi G}\delta Z_g\\ &+16C^2_{\varphi G}\delta Z_g + 8C_{\varphi G}C^{(3)}_{\varphi l}\delta Z_g - 4C_{\varphi G}C_{ll}\delta Z_g - C_{\varphi D}C_{\varphi G}\delta Z_h + 8C^2_{\varphi G}\delta Z_h + 4C_{\varphi G}C^{(3)}_{\varphi l}\delta Z_h\\ &-2C_{\varphi G}C_{ll}\delta Z_h + 4C_{\varphi\Box}C_{\varphi G}(-3\delta G_F+2\delta Z_g+\delta Z_h)\Big].\end{aligned} \tag{A2}$$

[4]We stress that we have not included unknown dimension-8 contributions that could also contribute at $\mathcal{O}(1/\Lambda^4)$.

The poles of δZ_h and δZ_g are respectively such that

$$\epsilon\delta Z_h\big|_{\rm poles} = \frac{2M_W^2 - 3m_t^2 + M_Z^2}{4\sqrt{2}\pi^2}G_F + \frac{1}{\Lambda^2}\left[\frac{3(M_Z^2 - M_W^2)}{4\pi^2}C_{\varphi B} + \frac{4M_W^2 + 2M_Z^2 - 7M_h^2 - 6m_t^2}{8\pi^2}C_{\varphi\Box} + \frac{5M_h^2 + 6m_t^2 - 4M_W^2 + M_Z^2}{32\pi^2}C_{\varphi D} + \frac{3m_t^2 - 2M_W^2 - M_Z^2}{4\pi^2}C_{\varphi l}^{(3)} + \frac{9M_W^2}{4\pi^2}C_{\varphi W} + \frac{3M_W\sqrt{M_Z^2 - M_W^2}}{4\pi^2}C_{\varphi WB} + \frac{M_Z^2 + 2M_W^2 - 3m_t^2}{8\pi^2}C_{ll} + \frac{3m_t}{4\sqrt{2}\pi^2(\sqrt{2}G_F)^{\frac{1}{2}}}C_{t\varphi}\right], \tag{A3}$$

$$\delta Z_g\big|_{\rm poles} = -\frac{5\alpha_s}{12\pi\epsilon_{\rm IR}} + \frac{1}{\epsilon_{\rm UV}}\left\{\frac{\alpha_s}{4\pi} + \frac{1}{\Lambda^2}\left[\frac{\sqrt{\alpha_s}m_t}{\sqrt{2}\pi^{\frac{3}{2}}(\sqrt{2}G_F)^{\frac{1}{2}}}C_{tG} - \frac{M_h^2 + 2M_W^2 + M_Z^2}{8\pi^2}C_{\varphi G}\right]\right\}. \tag{A4}$$

Finally, the counterterm $\delta C_{G^2\varphi^4}$ is

$$\epsilon\delta C_{G^2\varphi^4} = C_{\varphi G}^2\left\{\frac{3\sqrt{2}G_F M_h^2 + 28\alpha_s\pi}{8\pi^2}\right\} + C_{\varphi G}\left\{-\frac{3}{16\pi^2}C_H - \frac{3(\sqrt{2}G_F)^{\frac{1}{2}}m_t}{8\sqrt{2}\pi^2}C_{tH} - \frac{9G_F M_W^2}{4\sqrt{2}\pi^2}C_{\varphi W} + \frac{3G_F(m_t^2 - 2M_W^2)}{4\sqrt{2}\pi^2}C_{\varphi q}^{(3)} + \frac{3G_F(M_W - M_Z)(M_W + M_Z)}{4\sqrt{2}\pi^2}C_{\varphi B} - \frac{3G_F M_W\sqrt{M_Z^2 - M_W^2}}{4\sqrt{2}\pi^2}C_{\varphi WB} + \frac{G_F(45M_h^2 + 36m_t^2 - 46M_W^2 - 18M_Z^2)}{24\sqrt{2}\pi^2}C_{\varphi\Box} + \frac{3G_F(M_h^2 + 2m_t^2 - 2M_W^2 - M_Z^2)}{8\sqrt{2}\pi^2}C_{ll} + \frac{G_F(-3M_h^2 - 6m_t^2 + 4M_W^2 + 3M_Z^2)}{4\sqrt{2}\pi^2}C_{\varphi l}^{(3)} - \frac{G_F[13M_h^2 + 3(4m_t^2 - 8M_W^2 + M_Z^2)]}{32\sqrt{2}\pi^2}C_{\varphi D} + \frac{9\sqrt{\alpha_s}G_F M_h^2}{2\sqrt{2}\pi^{\frac{3}{2}}}C_G + \frac{\sqrt{\alpha_s}(\sqrt{2}G_F)^{\frac{1}{2}}m_t}{2\sqrt{2}\pi^{\frac{3}{2}}}C_{tG}\right\} + \frac{G_F m_t^2}{2\sqrt{2}\pi^2}C_{tG}^2 + \frac{\sqrt{\alpha_s}}{8\pi^{\frac{3}{2}}}C_{tG}C_{tH} + \frac{\sqrt{\alpha_s}(\sqrt{2}G_F)^{\frac{1}{2}}m_t}{2\sqrt{2}\pi^{\frac{3}{2}}}C_{\varphi l}^{(3)}C_{tG} - \frac{\sqrt{\alpha_s}(\sqrt{2}G_F)^{\frac{1}{2}}m_t}{4\sqrt{2}\pi^{\frac{3}{2}}}C_{ll}C_{tG} - \epsilon\delta C_{\varphi G}^8. \tag{A5}$$

APPENDIX B: FEYNMAN RULES

In this appendix, we collect all needed Feynman rules valid up to $\mathcal{O}(1/\Lambda^4)$. We adopt the notation of Ref. [37], but choose the WCs to be real and symmetric (e.g., $C_{f_2f_1}^{uG\star} = C_{f_2f_1}^{uG} \sim \delta_{f_1f_2}$). The remaining Feynman rules are only needed to $\mathcal{O}(1/\Lambda^2)$ in our calculation and can be found in Ref. [37]. For compactness, we present Feynman rules without inserting the field redefinitions of Eq. (12).

1. Quark-Higgs-gauge vertices

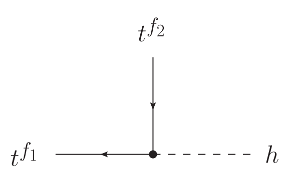

$$-\frac{i}{v_T}\delta_{f_1f_2}m_u R_\varphi^{-1} + \delta_{f_1f_2}\frac{iv_T^2C_{t\varphi}}{\sqrt{2}\Lambda^2}R_\varphi^{-1} \tag{B1}$$

2. Quark-gluon vertices

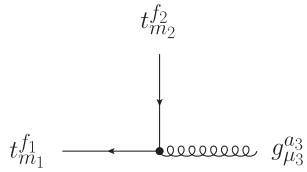

$$-i\bar{g}_s\delta_{f_1f_2}\mathcal{T}^{a_3}_{m_1m_2}\gamma^{\mu_3}-\sqrt{2}v_Tp_3^{\nu}\mathcal{T}^{a_3}_{m_1m_2}\sigma^{\mu_3\nu}\frac{C_{tG}}{\Lambda^2}R_g^{-1} \tag{B2}$$

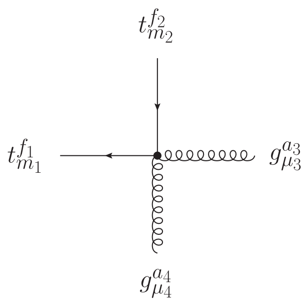

$$-i\sqrt{2}v_T\bar{g}_sf_{a_3a_4b_1}\mathcal{T}^{b_1}_{m_1m_2}\sigma^{\mu_3\mu_4}\frac{C_{tG}}{\Lambda^2}R_g^{-1} \tag{B3}$$

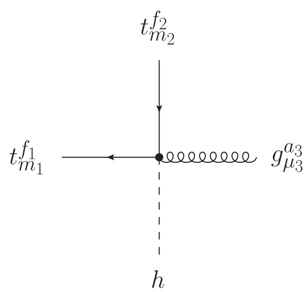

$$-\sqrt{2}p_3^{\nu}\mathcal{T}^{a_3}_{m_1m_2}\sigma^{\mu_3\nu}\frac{C_{tG}}{\Lambda^2}R_g^{-1}R_\varphi^{-1} \tag{B4}$$

3. Higgs-gauge vertices

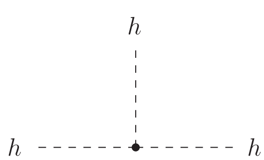

$$\begin{aligned}&-3i\lambda v_TR_\varphi^{-3}+\frac{15iv_T^3C_\varphi}{\Lambda^2}R_\varphi^{-3}-\frac{iv_TC_{\varphi D}}{\Lambda^2}R_\varphi^{-3}\big(p_1\cdot p_2+p_1\cdot p_3+p_2\cdot p_3\big)\\&-\frac{iv_TC_{\varphi\Box}}{\Lambda^2}R_\varphi^{-3}\big(3p_1^2+3p_2^2+3p_3^2+2p_1\cdot p_2+2p_1\cdot p_3+2p_2\cdot p_3\big)\end{aligned} \tag{B5}$$

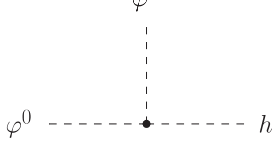

$$\begin{aligned}&-i\lambda v_TR_\varphi^{-1}R_{\varphi^0}^{-2}+\frac{3iv_T^3C_\varphi}{\Lambda^2}R_\varphi^{-1}R_{\varphi^0}^{-2}-\frac{iv_TC_{\varphi\Box}}{\Lambda^2}R_\varphi^{-1}R_{\varphi^0}^{-2}\left(p_1^2+p_2^2+p_3^2+2p_1\cdot p_2\right)\\&-\frac{iv_TC_{\varphi D}}{\Lambda^2}R_\varphi^{-1}R_{\varphi^0}^{-2}\left(p_1\cdot p_2\right)\end{aligned} \tag{B6}$$

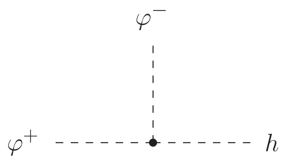

$$-i\lambda v_T R_\varphi^{-1} + \frac{3iv_T^3 C_\varphi}{\Lambda^2} R_\varphi^{-1} - \frac{iv_T C_{\varphi\Box}}{\Lambda^2} R_\varphi^{-1} \left(p_1 \cdot p_1 + 2p_1 \cdot p_2 + p_2 \cdot p_2 + p_3 \cdot p_3\right) - \frac{iv_T C_{\varphi D}}{2\Lambda^2} R_\varphi^{-1} (p_1 \cdot p_3 + p_2 \cdot p_3) \tag{B7}$$

4. Higgs-gluon vertices

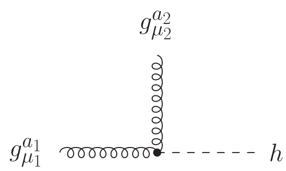

$$+4iv_T \delta_{a_1 a_2} \frac{C_{\varphi G}}{\Lambda^2} R_g^{-2} R_\varphi^{-1} \Big(p_1^{\mu_2} p_2^{\mu_1} - (p_1 \cdot p_2) g^{\mu_1 \mu_2}\Big) \tag{B8}$$

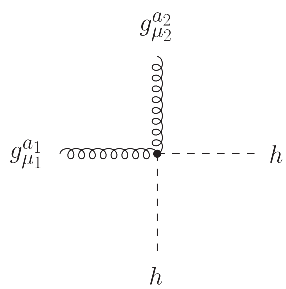

$$+4i\delta_{a_1 a_2} \frac{C_{\varphi G}}{\Lambda^2} R_g^{-2} R_\varphi^{-2} \Big(p_1^{\mu_2} p_2^{\mu_1} - (p_1 \cdot p_2) g^{\mu_1 \mu_2}\Big) \tag{B9}$$

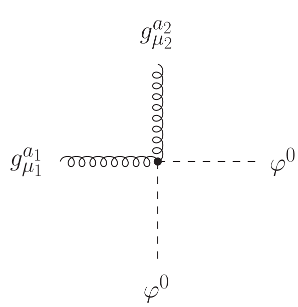

$$+4i\delta_{a_1 a_2} \frac{C_{\varphi G}}{\Lambda^2} R_g^{-2} R_{\varphi^0}^{-2} \Big(p_1^{\mu_2} p_2^{\mu_1} - (p_1 \cdot p_2) g^{\mu_1 \mu_2}\Big) \tag{B10}$$

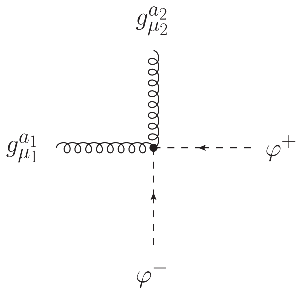

$$+4i\delta_{a_1a_2}\frac{C_{\varphi G}}{\Lambda^2}R_g^{-2}\Big(p_1^{\mu_2}p_2^{\mu_1}-(p_1\cdot p_2)g^{\mu_1\mu_2}\Big) \tag{B11}$$

5. Gluon-gluon vertices

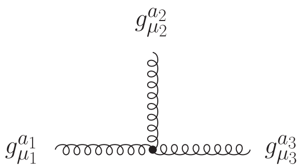

$$\begin{aligned}
&-\bar{g}_s f_{a_1a_2a_3}\left[\eta_{\mu_1\mu_2}(p_1-p_2)^{\mu_3}+\eta_{\mu_1\mu_3}(p_3-p_1)^{\mu_2}+\eta_{\mu_2\mu_3}(p_2-p_3)^{\mu_1}\right]\\
&+\frac{6C_G}{\Lambda^2}f_{a_1a_2a_3}R_g^{-3}\Big[p_3^{\mu_1}p_1^{\mu_2}p_2^{\mu_3}-p_2^{\mu_1}p_3^{\mu_2}p_1^{\mu_3}+\eta_{\mu_1\mu_2}(p_1^{\mu_3}(p_2\cdot p_3)-p_2^{\mu_3}(p_1\cdot p_3))\\
&\quad+\eta_{\mu_2\mu_3}(p_2^{\mu_1}(p_1\cdot p_3)-p_3^{\mu_1}(p_1\cdot p_2))+\eta_{\mu_3\mu_1}(p_3^{\mu_2}(p_1\cdot p_2)-p_1^{\mu_2}(p_2\cdot p_3))\Big]
\end{aligned} \tag{B12}$$

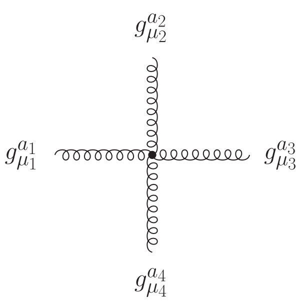

$$\begin{aligned}
&+i\bar{g}_s^2\Big(f_{a_1a_2b_1}f_{a_3a_4b_1}\,(\eta_{\mu_1\mu_4}\eta_{\mu_2\mu_3}-\eta_{\mu_1\mu_3}\eta_{\mu_2\mu_4})+f_{a_1a_3b_1}f_{a_2a_4b_1}\,(\eta_{\mu_1\mu_4}\eta_{\mu_2\mu_3}\\
&\quad-\eta_{\mu_1\mu_2}\eta_{\mu_3\mu_4})+f_{a_1a_4b_1}f_{a_2a_3b_1}\,(\eta_{\mu_1\mu_3}\eta_{\mu_2\mu_4}-\eta_{\mu_1\mu_2}\eta_{\mu_3\mu_4})\Big)\\
&-6i\bar{g}_s\frac{C_G}{\Lambda^2}R_g^{-3}\Big(f_{a_1a_2b_1}f_{a_3a_4b_1}[\eta_{\mu_1\mu_3}(p_1^{\mu_2}p_2^{\mu_4}+p_4^{\mu_2}p_3^{\mu_4})+\eta_{\mu_2\mu_4}(p_2^{\mu_1}p_1^{\mu_3}+p_3^{\mu_1}p_4^{\mu_3})\\
&\quad+\eta_{\mu_1\mu_2}(p_2^{\mu_3}p_1^{\mu_4}-p_1^{\mu_3}p_2^{\mu_4})+\eta_{\mu_3\mu_4}(p_4^{\mu_1}p_3^{\mu_2}-p_3^{\mu_1}p_4^{\mu_2})-\eta_{\mu_1\mu_4}(p_1^{\mu_2}p_2^{\mu_3}+p_3^{\mu_2}p_4^{\mu_3})\\
&\quad-\eta_{\mu_2\mu_3}(p_2^{\mu_1}p_1^{\mu_4}+p_4^{\mu_1}p_3^{\mu_4})+(\eta_{\mu_1\mu_4}\eta_{\mu_2\mu_3}-\eta_{\mu_1\mu_3}\eta_{\mu_2\mu_4})(p_1\cdot p_2+p_3\cdot p_4)]\\
&\quad+f_{a_1a_3b_1}f_{a_2a_4b_1}[\eta_{\mu_1\mu_2}(p_1^{\mu_3}p_3^{\mu_4}+p_4^{\mu_3}p_2^{\mu_4})+\eta_{\mu_3\mu_4}(p_3^{\mu_1}p_1^{\mu_2}+p_2^{\mu_1}p_4^{\mu_2})\\
&\quad+\eta_{\mu_1\mu_3}(p_3^{\mu_2}p_1^{\mu_4}-p_1^{\mu_2}p_3^{\mu_4})+\eta_{\mu_2\mu_4}(p_4^{\mu_1}p_2^{\mu_3}-p_2^{\mu_1}p_4^{\mu_3})-\eta_{\mu_1\mu_4}(p_3^{\mu_2}p_1^{\mu_3}+p_4^{\mu_2}p_2^{\mu_3})\\
&\quad-\eta_{\mu_2\mu_3}(p_3^{\mu_1}p_1^{\mu_4}+p_4^{\mu_1}p_2^{\mu_4})+(\eta_{\mu_1\mu_4}\eta_{\mu_2\mu_3}-\eta_{\mu_1\mu_2}\eta_{\mu_3\mu_4})(p_1\cdot p_3+p_2\cdot p_4)]\\
&\quad+f_{a_1a_4b_1}f_{a_2a_3b_1}[\eta_{\mu_1\mu_2}(p_2^{\mu_3}p_3^{\mu_4}+p_4^{\mu_3}p_1^{\mu_4})+\eta_{\mu_3\mu_4}(p_2^{\mu_1}p_3^{\mu_2}+p_4^{\mu_1}p_1^{\mu_2})\\
&\quad+\eta_{\mu_1\mu_4}(p_4^{\mu_2}p_1^{\mu_3}-p_1^{\mu_2}p_4^{\mu_3})+\eta_{\mu_2\mu_3}(p_3^{\mu_1}p_2^{\mu_4}-p_2^{\mu_1}p_3^{\mu_4})-\eta_{\mu_1\mu_3}(p_4^{\mu_2}p_1^{\mu_4}+p_3^{\mu_2}p_2^{\mu_4})\\
&\quad-\eta_{\mu_2\mu_4}(p_4^{\mu_1}p_1^{\mu_3}+p_3^{\mu_1}p_2^{\mu_3})+(\eta_{\mu_1\mu_3}\eta_{\mu_2\mu_4}-\eta_{\mu_1\mu_2}\eta_{\mu_3\mu_4})(p_1\cdot p_4+p_2\cdot p_3)]\Big)
\end{aligned} \tag{B13}$$

[1] The ATLAS Collaboration, Nature (London) **607**, 52 (2022).
[2] The CMS Collaboration, Nature (London) **607**, 60 (2022).
[3] J. de Blas *et al.*, J. High Energy Phys. 01 (2020) 139.
[4] I. Brivio and M. Trott, Phys. Rep. **793**, 1 (2019).
[5] J. J. Ethier, G. Magni, F. Maltoni, L. Mantani, E. R. Nocera, J. Rojo, E. Slade, E. Vryonidou, and C. Zhang (SMEFiT Collaboration), J. High Energy Phys. 11 (2021) 089.
[6] J. Ellis, M. Madigan, K. Mimasu, V. Sanz, and T. You, J. High Energy Phys. 04 (2021) 279.
[7] J. De Blas *et al.*, Eur. Phys. J. C **80**, 456 (2020).
[8] A. Biekoetter, T. Corbett, and T. Plehn, SciPost Phys. **6**, 064 (2019).
[9] S. Dawson, S. Homiller, and M. Sullivan, Phys. Rev. D **104**, 115013 (2021).
[10] S. Dawson, D. Fontes, S. Homiller, and M. Sullivan, Phys. Rev. D **106**, 055012 (2022).
[11] T. Corbett, A. Helset, A. Martin, and M. Trott, J. High Energy Phys. 06 (2021) 076.
[12] R. Boughezal, Y. Huang, and F. Petriello, Phys. Rev. D **106**, 036020 (2022).
[13] J. Ellis, H.-J. He, and R.-Q. Xiao, Phys. Rev. D **107**, 035005 (2023).
[14] S. Alioli *et al.*, in 2022 Snowmass Summer Study (2022), arXiv:2203.06771.
[15] R. Gomez Ambrosio, J. ter Hoeve, M. Madigan, J. Rojo, and V. Sanz, arXiv:2211.02058.
[16] G. Heinrich, J. Lang, and L. Scyboz, J. High Energy Phys. 08 (2022) 079.
[17] L. Allwicher, D. A. Faroughy, F. Jaffredo, O. Sumensari, and F. Wilsch, arXiv:2207.10714.
[18] E. da Silva Almeida, A. Alves, N. Rosa Agostinho, O. J. P. Éboli, and M. C. Gonzalez-Garcia, Phys. Rev. D **99**, 033001 (2019).
[19] S. Dawson and P. P. Giardino, Phys. Rev. D **101**, 013001 (2020).
[20] L. Berthier and M. Trott, J. High Energy Phys. 05 (2015) 024.
[21] I. Brivio, J. High Energy Phys. 04 (2021) 073.
[22] C. Degrande, G. Durieux, F. Maltoni, K. Mimasu, E. Vryonidou, and C. Zhang, Phys. Rev. D **103**, 096024 (2021).
[23] J. Baglio, S. Dawson, S. Homiller, S. D. Lane, and I. M. Lewis, Phys. Rev. D **101**, 115004 (2020).
[24] C. Hays, A. Martin, V. Sanz, and J. Setford, J. High Energy Phys. 02 (2019) 123.
[25] R. Contino, A. Falkowski, F. Goertz, C. Grojean, and F. Riva, J. High Energy Phys. 07 (2016) 144.
[26] C. Anastasiou, C. Duhr, F. Dulat, E. Furlan, T. Gehrmann, F. Herzog, A. Lazopoulos, and B. Mistlberger, J. High Energy Phys. 05 (2016) 058.
[27] B. Mistlberger, J. High Energy Phys. 05 (2018) 028.
[28] J. Baglio, C. Duhr, B. Mistlberger, and R. Szafron, J. High Energy Phys. 12 (2022) 066.
[29] C. Degrande, J. M. Gerard, C. Grojean, F. Maltoni, and G. Servant, J. High Energy Phys. 07 (2012) 036; 03 (2013) 32(E).
[30] F. Maltoni, E. Vryonidou, and C. Zhang, J. High Energy Phys. 10 (2016) 123.
[31] M. Grazzini, A. Ilnicka, M. Spira, and M. Wiesemann, J. High Energy Phys. 03 (2017) 115.
[32] N. Deutschmann, C. Duhr, F. Maltoni, and E. Vryonidou, J. High Energy Phys. 12 (2017) 063; 02 (2018) 159(E).
[33] R. V. Harlander and T. Neumann, Phys. Rev. D **88**, 074015.
[34] T. Corbett, A. Martin, and M. Trott, J. High Energy Phys. 12 (2021) 147.
[35] A. Martin and M. Trott, Phys. Rev. D **105**, 076004 (2022).
[36] B. Grzadkowski, M. Iskrzynski, M. Misiak, and J. Rosiek, J. High Energy Phys. 10 (2010) 085.
[37] A. Dedes, W. Materkowska, M. Paraskevas, J. Rosiek, and K. Suxho, J. High Energy Phys. 06 (2017) 143.
[38] C. W. Murphy, J. High Energy Phys. 10 (2020) 174.
[39] H.-L. Li, Z. Ren, J. Shu, M.-L. Xiao, J.-H. Yu, and Y.-H. Zheng, Phys. Rev. D **104**, 015026 (2021).
[40] S. Das Bakshi, M. Chala, A. Díaz-Carmona, and G. Guedes, Eur. Phys. J. Plus **137**, 973 (2022).
[41] M. Chala, G. Guedes, M. Ramos, and J. Santiago, SciPost Phys. **11**, 065 (2021).
[42] A. Helset, E. E. Jenkins, and A. V. Manohar, J. High Energy Phys. 02 (2023) 063.
[43] M. Chala, A. Díaz-Carmona, and G. Guedes, J. High Energy Phys. 05 (2022) 138.
[44] G. L. De Sousa Fihalo Guedes, A global approach to physics beyond the Standard Model, Ph.D. thesis, Granada University, 2022.
[45] D. Fontes and J. C. Romão, Comput. Phys. Commun. **256**, 107311 (2020).
[46] D. Fontes and J. C. Romão, J. High Energy Phys. 06 (2021) 016.
[47] N. D. Christensen and C. Duhr, Comput. Phys. Commun. **180**, 1614 (2009).
[48] A. Alloul, N. D. Christensen, C. Degrande, C. Duhr, and B. Fuks, Comput. Phys. Commun. **185**, 2250 (2014).
[49] P. Nogueira, J. Comput. Phys. **105**, 279 (1993).
[50] R. Mertig, M. Bohm, and A. Denner, Comput. Phys. Commun. **64**, 345 (1991).
[51] V. Shtabovenko, R. Mertig, and F. Orellana, Comput. Phys. Commun. **207**, 432 (2016).
[52] V. Shtabovenko, R. Mertig, and F. Orellana, Comput. Phys. Commun. **256**, 107478 (2020).
[53] V. Shtabovenko, Comput. Phys. Commun. **218**, 48 (2017).
[54] D. Fontes, Multi-Higgs models: Model building, phenomenology and renormalization, Ph.D. thesis, University of Lisbon, 2021.
[55] A. Denner, Fortschr. Phys. **41**, 307 (1993).
[56] A. Denner, S. Dittmaier, and J.-N. Lang, J. High Energy Phys. 11 (2018) 104.
[57] G. 't Hooft, Nucl. Phys. **B61**, 455 (1973).
[58] S. Weinberg, Phys. Rev. D **8**, 3497 (1973).
[59] S. Catani, Phys. Lett. B **427**, 161 (1998).
[60] H. H. Patel, Comput. Phys. Commun. **197**, 276 (2015).
[61] H. H. Patel, Comput. Phys. Commun. **218**, 66 (2017).
[62] S. Dawson and P. P. Giardino, Phys. Rev. D **97**, 093003 (2018).
[63] E. E. Jenkins, A. V. Manohar, and M. Trott, J. High Energy Phys. 10 (2013) 087.

[64] E. E. Jenkins, A. V. Manohar, and M. Trott, J. High Energy Phys. 01 (2014) 035.
[65] R. Alonso, E. E. Jenkins, A. V. Manohar, and M. Trott, J. High Energy Phys. 04 (2014) 159.
[66] J. de Blas, J. C. Criado, M. Perez-Victoria, and J. Santiago, J. High Energy Phys. 03 (2018) 109.
[67] See Supplemental Material at http://link.aps.org/supplemental/10.1103/PhysRevD.107.055038 contains analytical results for F_{V} [defined in Eq. (23)].